

Solving SU(3) Yang-Mills theory on the lattice: a calculation of selected gauge observables with gradient flow

Hans Mathias Mamen Vege

May 12, 2019

Supervisor: *Andrea Shindler*

Co-supervisor: *Morten Hjorth-Jensen*

University of Oslo

Introduction

Structure

- Quantum Chromodynamics(QCD).

- **QCD.** We will go through and explain what QCD as well as motivate its existence.

Structure

- Quantum Chromodynamics(QCD).
- Lattice QCD.

1

- **QCD.** We will go through and explain what QCD as well as motivate its existence.
- **LQCD.** We will briefly show how one discretise the lattice and perform calculations on it.

Structure

- Quantum Chromodynamics(QCD).
- Lattice QCD.
- Gradient flow.

1

- **QCD.** We will go through and explain what QCD as well as motivate its existence.
- **LQCD.** We will briefly show how one discretise the lattice and perform calculations on it.
- **Gradient flow.** We will quickly introduce gradient flow and explain its effects.

Structure

- Quantum Chromodynamics(QCD).
- Lattice QCD.
- Gradient flow.
- Developing a code for solving $SU(3)$ Yang-Mills theory.

1

- **QCD.** We will go through and explain what QCD as well as motivate its existence.
- **LQCD.** We will briefly show how one discretise the lattice and perform calculations on it.
- **Gradient flow.** We will quickly introduce gradient flow and explain its effects.
- **GLAC.** Will briefly present the code which we developed as well as some benchmarks. We will also present the Metropolis algorithm.

Structure

- Quantum Chromodynamics(QCD).
- Lattice QCD.
- Gradient flow.
- Developing a code for solving $SU(3)$ Yang-Mills theory.
- Results.

1

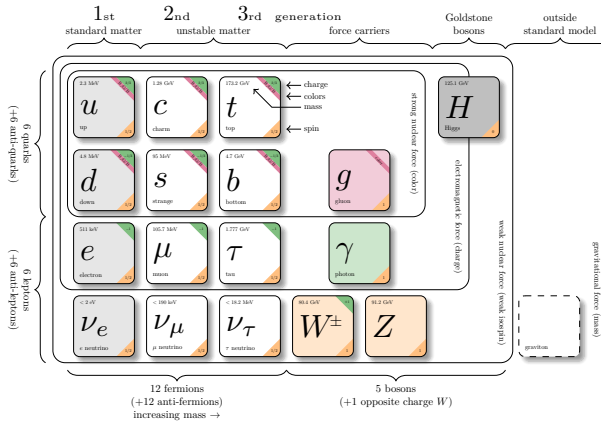
- **QCD.** We will go through and explain what QCD as well as motivate its existence.
- **LQCD.** We will briefly show how one discretise the lattice and perform calculations on it.
- **Gradient flow.** We will quickly introduce gradient flow and explain its effects.
- **GLAC.** Will briefly present the code which we developed as well as some benchmarks. We will also present the Metropolis algorithm.
- **Results.** We will present the results obtained from pure gauge calculations.

Structure

- Quantum Chromodynamics(QCD).
- Lattice QCD.
- Gradient flow.
- Developing a code for solving $SU(3)$ Yang-Mills theory.
- Results.

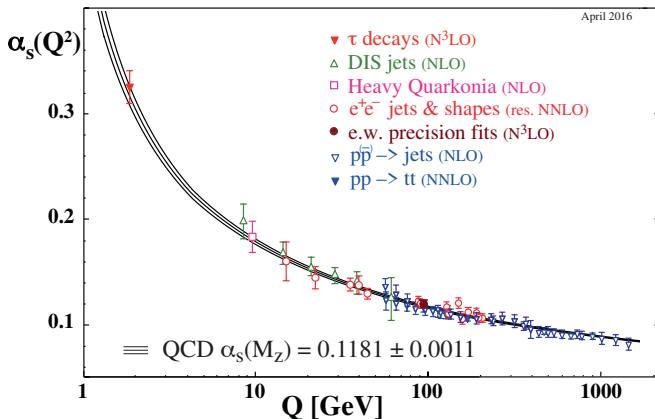
Quantum Chromodynamics(QCD)

The Standard Model



Consists of the innermost square of the six quarks and the gluons.

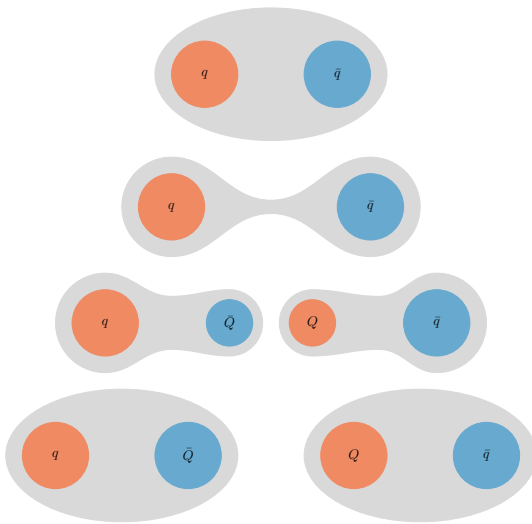
Asymptotic freedom



3

- The coupling constant **decreases** as we **increase** the energy
- One of the experimental proofs of QCD along with triple γ decay and muon cross section ratio R . **LEGE TIL MER HER!! EVT FJERNE.**
OPPSUMMER MER!

Confinement



4

If we try to pull apart **two quarks in a meson**, more and more energy is required until we have enough energy to spontaneously create a **quark-antiquark pair**, forming thus **two new mesons**.

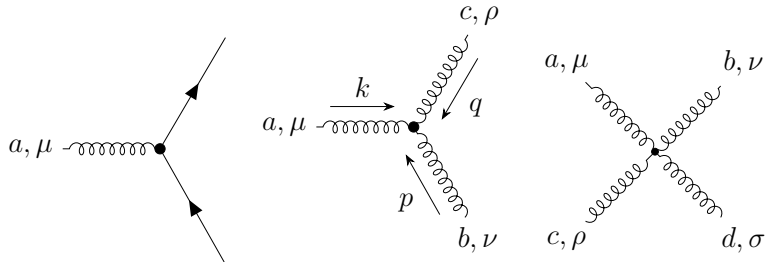
The non-linearity of QCD

The QCD Lagrangian

$$\mathcal{L}_{\text{QCD}} = \sum_{f=1}^{N_f} \bar{\psi}^{(f)} \left(i \not{D} - m^{(f)} \right) \psi^{(f)} - \frac{1}{4} G_{\mu\nu}^a G^{a\mu\nu},$$

with action

$$S = \int d^4x \mathcal{L}_{\text{QCD}}. \quad (1)$$



Topology in QCD

- Instantons

- **Instantons** are local minimums to the Yang-Mills action in Euclidean space.

Topology in QCD

- Instantons
- Topological charge, Q

6

- **Instantons** are local minimums to the Yang-Mills action in Euclidean space.
- Measuring **topological charge** is a measure of the *Winding number* of the gauge field.

Topology in QCD

- Instantons
- Topological charge, Q
- Winding number

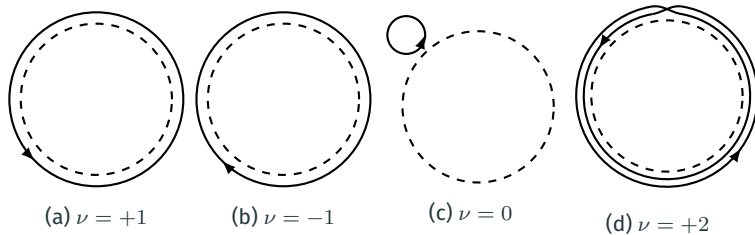


Figure 1: The figure is taken from Forkel [3, p. 32].

6

- **Instantons** are local minimums to the Yang-Mills action in Euclidean space.
- Measuring **topological charge** is a measure of the *Winding number* of the gauge field.
- An illustration of how one can view the winding number given a function f that parametrizes a path around a circle S^1 . Given that it starts and ends at the same point, we have that the number of times it wraps around the circle gives us the winding number.

Topology in QCD

- Instantons
- Topological charge, Q
- Winding number

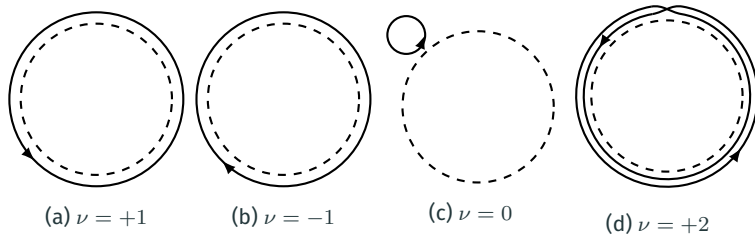


Figure 1: The figure is taken from Forkel [3, p. 32].

6

- **Instantons** are local minimums to the Yang-Mills action in Euclidean space.
- Measuring **topological charge** is a measure of the *Winding number* of the gauge field.
- An illustration of how one can view the winding number given a function f that parametrizes a path around a circle S^1 . Given that it starts and ends at the same point, we have that the number of times it wraps around the circle gives us the winding number.

The Witten-Veneziano relation

A formula connecting pure gauge theory and full QCD.

$$m_{\eta'}^2 = \frac{2N_f}{f_\pi^2} \chi_{\text{top}} \quad (2)$$

- Pion decay constant $f_\pi = 0.130(5)/\sqrt{2}$ GeV.
- η' meson mass $m_{\eta'} = 0.95778(6)$ GeV.
- χ_{top} is the *topological susceptibility*.

MORE ON WV FORMULA. CLARIFY WHAT IT IS AND WHAT IT EXPLAINS.

- We use the experimental values for the pion decay constant and the η' mass.
- Allows us to estimate the number of flavors in our theory N_f .
- χ_{top} is the topological susceptibility, calculated from the expectation value of Q .

Lattice Quantum Chromodynamics(LQCD)

Discretizing spacetime

1. Divide spacetime into a cube of size $N^3 \times N_T$.

Discretizing spacetime

1. Divide spacetime into a cube of size $N^3 \times N_T$.
2. Fermions live on the each *point* in the cube.

Discretizing spacetime

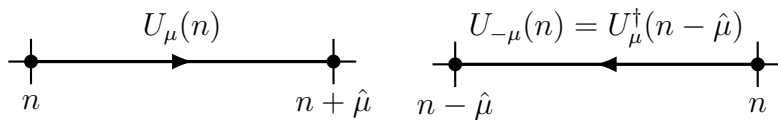
1. Divide spacetime into a cube of size $N^3 \times N_T$.
2. Fermions live on the each *point* in the cube.
3. The gauge fields live on the sites *in between* the points, and is called links.

Links

A link

$$U_\mu(n) = \exp [iaA_\mu(n)],$$

connects one lattice site to another and is a $SU(3)$ matrix.



where $U_{-\mu}(n) = U_\mu(n - \hat{\mu})^\dagger$.

- Defined from the gauge transporter.
- A link in the positive $\hat{\mu}$ direction is shown in the figure to the left.
- A link in the negative $\hat{\mu}$ direction is shown in the figure to the right.

Gauge invariance on the lattice

Links gauge transform as

$$U_\mu(n) \rightarrow U'_\mu(n) = \Omega(n) U_\mu(n) \Omega(n + \hat{\mu})^\dagger,$$
$$U_{-\mu}(n) \rightarrow U'_{-\mu}(n) = \Omega(n) U_\mu(n - \hat{\mu})^\dagger \Omega(n - \hat{\mu})^\dagger.$$

Gauge invariance on the lattice

Links gauge transform as

$$U_\mu(n) \rightarrow U'_\mu(n) = \Omega(n) U_\mu(n) \Omega(n + \hat{\mu})^\dagger,$$
$$U_{-\mu}(n) \rightarrow U'_{-\mu}(n) = \Omega(n) U_\mu(n - \hat{\mu})^\dagger \Omega(n - \hat{\mu})^\dagger.$$

Two main types of gauge invariant objects,

Gauge invariance on the lattice

Links gauge transform as

$$U_\mu(n) \rightarrow U'_\mu(n) = \Omega(n) U_\mu(n) \Omega(n + \hat{\mu})^\dagger,$$
$$U_{-\mu}(n) \rightarrow U'_{-\mu}(n) = \Omega(n) U_\mu(n - \hat{\mu})^\dagger \Omega(n - \hat{\mu})^\dagger.$$

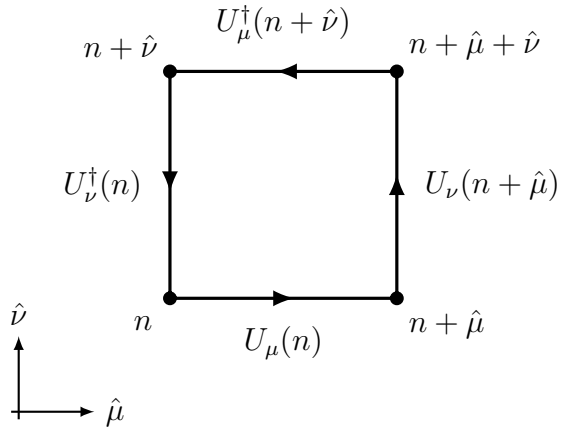
Two main types of gauge invariant objects,

- Fully connected gauge invariant objects.
- Objects with fermions $\psi, \bar{\psi}$ as end points.

The plaquette

The simplest gauge invariant object,

$$\begin{aligned} P_{\mu\nu}(n) &= U_\mu(n) U_\nu(n + \hat{\mu}) U_{-\mu}(n + \hat{\mu} + \hat{\nu}) U_{-\nu}(n + \hat{\nu}) \\ &= U_\mu(n) U_\nu(n + \hat{\mu}) U_\mu(n + \hat{\nu})^\dagger U_\nu(n)^\dagger, \end{aligned}$$



The Wilson gauge action

The Wilson gauge action is given as

$$S_G[U] = \frac{\beta}{3} \sum_{n \in \Lambda} \sum_{\mu < \nu} \text{Re} \operatorname{tr} [1 - P_{\mu\nu}(n)], \quad (3)$$

with $\beta = 6/g_S^2$.

- Using the definition of the link we saw earlier, we can reproduce the continuum action up to a discretization error of $\mathcal{O}(a^2)$.

Developing a code for solving SU(3) Yang-Mills theory on the lattice

The numerical challenge in lattice QCD

A lattice configuration consists of SU(3) matrices,

13

- The SU(3) matrices are 3×3 matrices of nine complex numbers or 18 real numbers.
- This leads to an absolute **requirement of efficiency**, both in **calculations** and in **input/output**.
- When returning to what ensembles of configurations we generated this will be evident.

The numerical challenge in lattice QCD

A lattice configuration consists of SU(3) matrices,

$$\underbrace{N^3}_{\text{Spatial}} \times \underbrace{N_T}_{\text{Temporal}} \times \underbrace{4}_{\text{Links}} \times \underbrace{9}_{\text{SU(3) matrix}} \times \underbrace{2}_{\mathbb{C}\text{-numbers}} = 72N^3N_T,$$

13

- The SU(3) matrices are 3×3 matrices of nine complex numbers or 18 real numbers.
- This leads to an absolute **requirement of efficiency**, both in **calculations** and in **input/output**.
- When returning to what ensembles of configurations we generated this will be evident.

The numerical challenge in lattice QCD

A lattice configuration consists of $SU(3)$ matrices,

$$\underbrace{N^3}_{\text{Spatial}} \times \underbrace{N_T}_{\text{Temporal}} \times \underbrace{4}_{\text{Links}} \times \underbrace{9}_{\text{\text{SU}(3) matrix}} \times \underbrace{2}_{\mathbb{C}\text{-numbers}} = 72N^3N_T,$$

$\rightarrow 8 \times 72N^3N_T$ bytes.

13

- The $SU(3)$ matrices are 3×3 matrices of nine complex numbers or 18 real numbers.
- This leads to an absolute **requirement of efficiency**, both in **calculations** and in **input/output**.
- When returning to what ensembles of configurations we generated this will be evident.

The path integral I

$$\langle O \rangle = \frac{1}{Z} \int \mathcal{D}U O[\psi, \bar{\psi}, U] e^{-S_G[U] - S_F[\psi, \bar{\psi}, U]}.$$

MOVE PATH INTEGRAL FIGURE TO THIS LOCATION TO ILLUSTRATE WHAT A PATH INTEGRAL IS!with

$$Z = \int \mathcal{D}U \mathcal{D}\bar{\psi} \mathcal{D}\psi e^{-S_G[U] - S_F[\psi, \bar{\psi}, U]}.$$

PRESENT METROPOLIS ALGORITHM AFTER SHOWING THE PATH INTEGRAL?

The path integral I

$$\langle O \rangle = \frac{1}{Z} \int \mathcal{D}U O[U] e^{-S_G[U]}.$$

MOVE PATH INTEGRAL FIGURE TO THIS LOCATION TO ILLUSTRATE WHAT A PATH INTEGRAL IS!with

$$Z = \int \mathcal{D}U e^{-S_G[U]}.$$

PRESENT METROPOLIS ALGORITHM AFTER SHOWING THE PATH INTEGRAL?

The path integral I

MOVE PATH INTEGRAL FIGURE TO THIS LOCATION TO ILLUSTRATE WHAT A PATH INTEGRAL IS!

$$\langle O \rangle = \frac{1}{Z} \int \mathcal{D}U O[U] e^{-S_G[U]}.$$

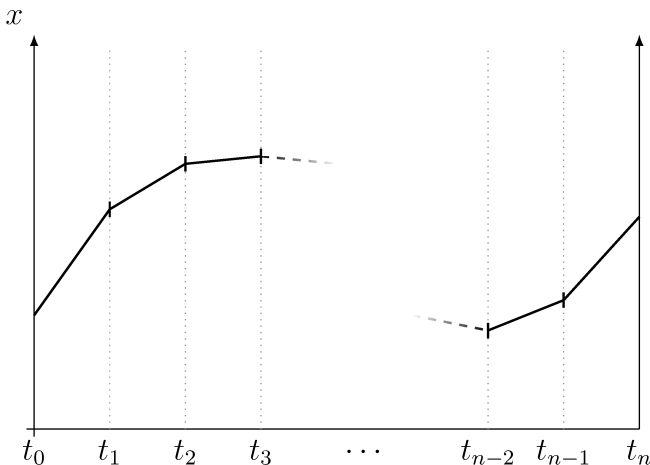
with

$$Z = \int \mathcal{D}U e^{-S_G[U]}.$$

PRESENT METROPOLIS ALGORITHM AFTER SHOWING THE PATH INTEGRAL?

The path integral II

MOVE THIS FIGURE TO BEING THE FIRST SLIDE WHEN PRESENTING PATH INTEGRALS, AS IT REALLY DOES NOT SHOW LATTICE PATH INTEGRALS



An example of the discretized path integral, going from time t_0 to t_n , where the end points is taken to be equal, $x_0 = x_{N_T}$. We integrate over all of space at each time t_i finding the most likely position at a given time.

How to measure

The observable becomes an average over the N_{MC} gauge configurations.

$$\langle O \rangle = \lim_{N_{\text{MC}} \rightarrow \infty} \frac{1}{N_{\text{MC}}} \sum_i^{N_{\text{MC}}} O[U_i]$$

We now need to generate configurations...

- We perform an average of the created configurations.

The Metropolis algorithm

MAYBE SKIP SLIDE THIS??

repeat

 Randomly generate a candidate state j with probability $T_{i \rightarrow j}$.

 Calculate $A_{i \rightarrow j}$ which saw on previous slide.

 Generate random number $u \in [0, 1]$.

if $u \leq A_{i \rightarrow j}$ **then**

 Accept new state j .

else if $u > A_{i \rightarrow j}$ **then**

 Reject new state j and retain the old state i .

end if

until N_{MC} samples are generated.

- Generated state j is a gauge configuration.
- Algorithm of choice when sampling gauge configurations.
- For generating N_{MC} Monte Carlo samples.

The Metropolis algorithm on the lattice

A parameter ϵ_{rnd} controls the spread of the candidate matrices.

1. Initialize lattice with SU(3) matrices close to unity(*hot start*) or at unity(*cold start*).
2. Thermalize with N_{therm} sweeps.
3. Generate N_{MC} samples,
 - i Perform N_{corr} correlation updates.
 - ii At each update, perform N_{up} single link update for every lattice link.
 - iii Store configuration and/or apply gradient flow and sample observables on it.

- We use **periodic boundary conditions** for all calculations.
- N_{MC} is how many configurations we will generate.
- N_{up} is how many single link updates we will perform.
- N_{corr} is how many full sweeps we shall perform in between each sampling. Needed in order to reduce the autocorrelation between the configurations.
- We checked that our choice for the matrix generation parameter ϵ_{rnd} minimizes the autocorrelation.

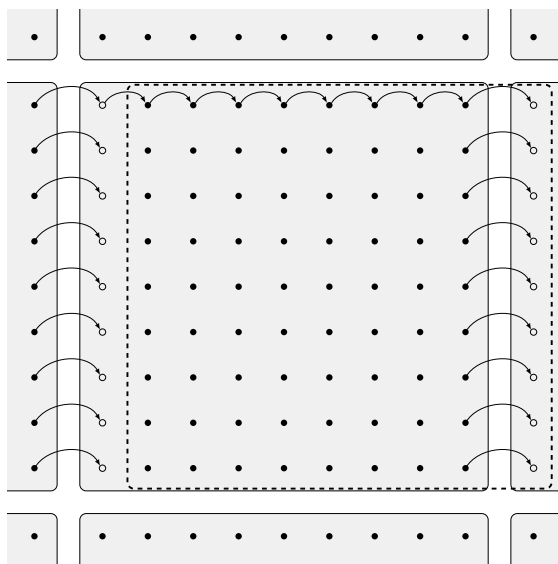
Parallelization

Two methods used:

- Single link sharing used in the Metropolis algorithm.
- *shifts* used in gradient flow and observable sampling

- Tested out **halos**, but turned out to be problematic when generating.
- We parallelized using MPI.

Shifts



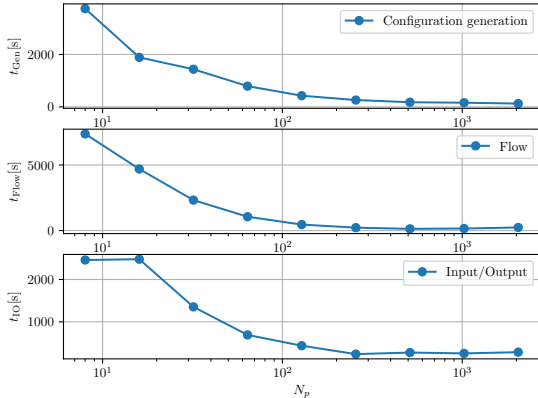
20

- An illustration of the lattice shift.
- The links U_ν of the lattice are copied over to a temporary lattice shifted in direction $\hat{\mu}$.
- The face that is shifted over to an adjacent sub-lattice is shared through a non-blocking MPI call, while we copy the links to the temporary lattice.
- Allows for a simplified syntax close to that of the equations we are working with.
- Don't have to write out any loops over the lattice positions.

Scaling

We checked three types of scaling,

- Strong scaling: *fixed problem* and a variable N_p cores



21

- Strong scaling

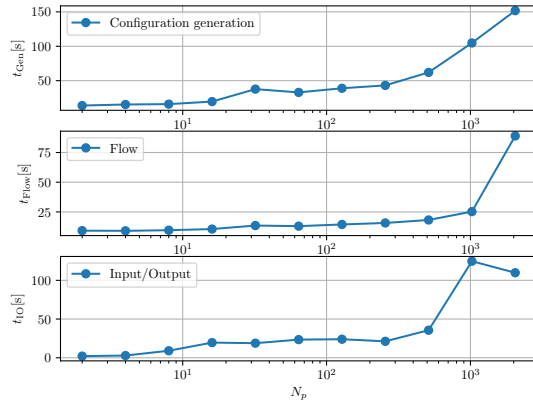
FIX THE SLIDES HERE!

FINAL <3-> is redundant!!

Scaling

We checked three types of scaling,

- **Strong scaling:** fixed problem and a variable N_p cores
- **Weak scaling:** fixed problem per processor and a variable N_p cores.



21

- Strong scaling

FIX THE SLIDES HERE!

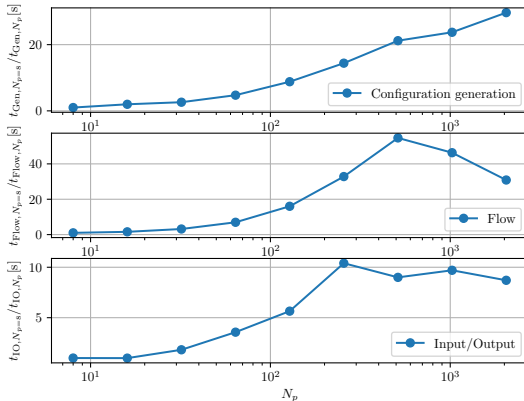
FINAL v3 > is redundant!!

Weak scaling

Scaling

We checked three types of scaling,

- **Strong scaling:** fixed problem and a variable N_p cores
- **Weak scaling:** fixed problem per processor and a variable N_p cores.
- **Speedup:** defined as $S(p) = \frac{t_{N_p=0}}{t_{N_p}}$.



21

We Strong scaling have a plateau around 512 cores. **FIX THE SLIDES HERE!**
FINAL <3> is redundant!!

- The speedup of the configuration generation, flowing, and IO. The speedup is calculated by dividing the run time of each N_p run, with the run time of the run with the least number of processors, $N_p = 8$.

Scaling

We checked three types of scaling,

- **Strong scaling:** *fixed problem and a variable N_p cores*
- **Weak scaling:** *fixed problem per processor and a variable N_p cores.*
- **Speedup:** defined as $S(p) = \frac{t_{N_p,0}}{t_{N_p}}$.

We appear to have a plateau around 512 cores. **FIX THE SLIDES HERE!**
FINAL <3-> is redundant!!

21

- Strong scaling
- Weak scaling
- The speedup of the configuration generation, flowing, and IO. The speedup is calculated by dividing the run time of each N_p run, with the run time of the run with the least number of processors, $N_p = 8$.
- The IO was optimized later to be a factor of ten or more faster.

Scaling

We checked three types of scaling,

- **Strong scaling:** *fixed problem and a variable N_p cores*
- **Weak scaling:** *fixed problem per processor and a variable N_p cores.*
- **Speedup:** defined as $S(p) = \frac{t_{N_p,0}}{t_{N_p}}$.

We appear to have a plateau around 512 cores. **FIX THE SLIDES HERE!**
FINAL <3-> is redundant!!

21

- Strong scaling
- Weak scaling
- The speedup of the configuration generation, flowing, and IO. The speedup is calculated by dividing the run time of each N_p run, with the run time of the run with the least number of processors, $N_p = 8$.
- The IO was optimized later to be a factor of ten or more faster.

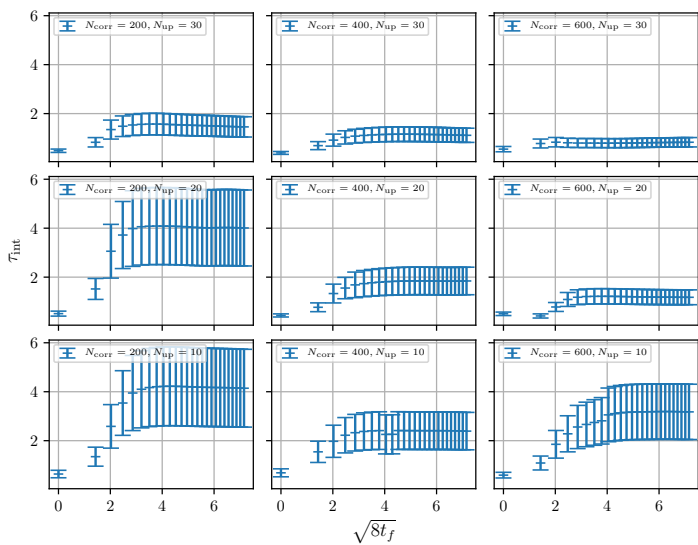
Optimizing the gauge configuration generation

Generated 200 configurations for a lattice of size $N^3 \times N_T = 16^3 \times 32$ and $\beta = 6.0$, for combinations of $N_{\text{corr}} \in [200, 400, 600]$ and $N_{\text{up}} \in [10, 20, 30]$.

22

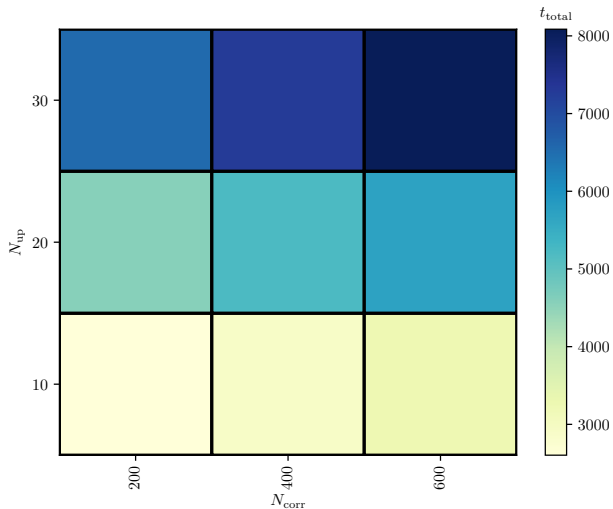
- We run for different values for N_{up} and N_{corr} to see what gives optimizes **computational cost** and **autocorrelation**.
- The integrated autocorrelation time for topological charge $\langle Q \rangle$ for a lattice of size $N = 16$ and $N_T = 32$ with $\beta = 6.0$ for combinations of $N_{\text{corr}} \in [200, 400, 600]$ and $N_{\text{up}} \in [10, 20, 30]$, plotted against flow time $\sqrt{8t_f}$.

Optimizing the gauge configuration generation



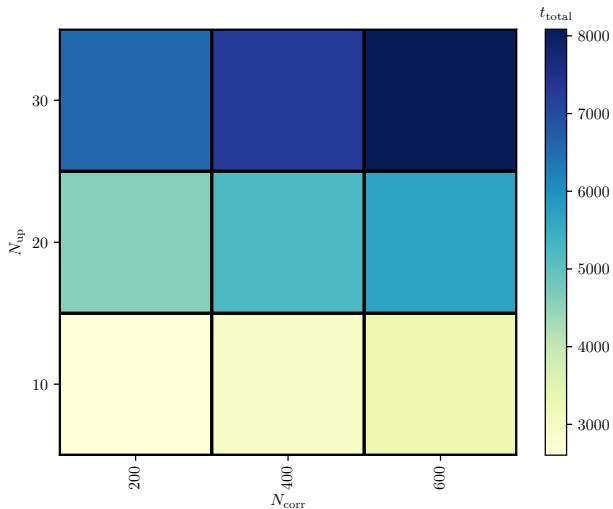
- The time taking to generate 200 configurations and flowing them $N_{\text{flow}} = 250$ flow steps for a lattice of size $N = 16$ and $N_T = 32$, with $\beta = 6.0$ for combinations of $N_{\text{corr}} \in [200, 400, 600]$ and $N_{\text{up}} \in [10, 20, 30]$.

Optimizing the gauge configuration generation



- What we see is that increasing N_{up} is a cheaper alternative compared to using N_{corr}

Optimizing the gauge configuration generation



- What we see is that increasing N_{up} is a cheaper alternative compared to using N_{corr}

Verifying the code

- Unit testing. SU(3), SU(2) multiplications.

Verifying the code

- **Unit testing.** SU(3), SU(2) multiplications.
- **Integration testing.** Random matrix generation, lattice objects, parallelization, ect.

Verifying the code

- **Unit testing.** SU(3), SU(2) multiplications.
- **Integration testing.** Random matrix generation, lattice objects, parallelization, ect.
- **Validation testing.** Cross checking results with a configuration from Chroma.

Gradient flow

The flow equation

The flow of the SU(3) gauge fields are denoted by $B_\mu(x, t_f)$ which are Lie algebra valued gauge fields,

$$\frac{d}{dt_f} B_\mu(x, t_f) = D_\nu G_{\nu \mu}(x, t_f), \quad (4)$$

- The flow equation in the continuum is defined by this differential equation.

The flow equation

The flow of the SU(3) gauge fields are denoted by $B_\mu(x, t_f)$ which are Lie algebra valued gauge fields,

$$\frac{d}{dt_f} B_\mu(x, t_f) = D_\nu G_{\nu \mu}(x, t_f), \quad (4)$$

$$D_\mu = \partial_\mu + [B_\mu(x, t_f), \cdot], \quad (5)$$

- The flow equation in the continuum is defined by this differential equation.
- With the covariant derivative given by following, with the \cdot being the derivative with respect to flow time.

The flow equation

The flow of the SU(3) gauge fields are denoted by $B_\mu(x, t_f)$ which are Lie algebra valued gauge fields,

$$\frac{d}{dt_f} B_\mu(x, t_f) = D_\nu G_{\nu \mu}(x, t_f), \quad (4)$$

$$D_\mu = \partial_\mu + [B_\mu(x, t_f), \cdot], \quad (5)$$

$$G_{\mu\nu}(x, t_f) = \partial_\mu B_\nu(x, t_f) - \partial_\nu B_\mu(x, t_f) - i[B_\mu(x, t_f), B_\nu(x, t_f)], \quad (6)$$

- The flow equation in the continuum is defined by this differential equation.
- With the covariant derivative given by following, with the \cdot being the derivative with respect to flow time.
- The field strength tensor of the flown fields is given in the regular format.

The flow equation

The flow of the SU(3) gauge fields are denoted by $B_\mu(x, t_f)$ which are Lie algebra valued gauge fields,

$$\frac{d}{dt_f} B_\mu(x, t_f) = D_\nu G_{\nu \mu}(x, t_f), \quad (4)$$

$$D_\mu = \partial_\mu + [B_\mu(x, t_f), \cdot], \quad (5)$$

$$G_{\mu\nu}(x, t_f) = \partial_\mu B_\nu(x, t_f) - \partial_\nu B_\mu(x, t_f) - i[B_\mu(x, t_f), B_\nu(x, t_f)], \quad (6)$$

with the initial conditions being the fundamental gauge field,

$$B_\mu(x, t_f)|_{t_f=0} = A_\mu(x).$$

- The flow equation in the continuum is defined by this differential equation.
- With the covariant derivative given by following, with the \cdot being the derivative with respect to flow time.
- The field strength tensor of the flown fields is given in the regular format.
- The initial condition is the un-flowed gauge field, A_μ .

The flow equation

The flow of the SU(3) gauge fields are denoted by $B_\mu(x, t_f)$ which are Lie algebra valued gauge fields,

$$\frac{d}{dt_f} B_\mu(x, t_f) = D_\nu G_{\nu \mu}(x, t_f), \quad (4)$$

$$D_\mu = \partial_\mu + [B_\mu(x, t_f), \cdot], \quad (5)$$

$$G_{\mu\nu}(x, t_f) = \partial_\mu B_\nu(x, t_f) - \partial_\nu B_\mu(x, t_f) - i[B_\mu(x, t_f), B_\nu(x, t_f)], \quad (6)$$

with the initial conditions being the fundamental gauge field,

$$B_\mu(x, t_f)|_{t_f=0} = A_\mu(x).$$

A bad approximation: *the diffusion equation*,

$$\frac{\partial}{\partial t_f} B_\mu(x, t_f) \approx \partial^2 B_\mu(x, t_f)$$

24

- The flow equation in the continuum is defined by this differential equation.
- With the covariant derivative given by following, with the \cdot being the derivative with respect to flow time.
- The field strength tensor of the flown fields is given in the regular format.
- The initial condition is the un-flowed gauge field, A_μ .
- Bad approx.: diffusion equation.

The flow equation

The flow of the SU(3) gauge fields are denoted by $B_\mu(x, t_f)$ which are Lie algebra valued gauge fields,

$$\frac{d}{dt_f} B_\mu(x, t_f) = D_\nu G_{\nu \mu}(x, t_f), \quad (4)$$

$$D_\mu = \partial_\mu + [B_\mu(x, t_f), \cdot], \quad (5)$$

$$G_{\mu\nu}(x, t_f) = \partial_\mu B_\nu(x, t_f) - \partial_\nu B_\mu(x, t_f) - i[B_\mu(x, t_f), B_\nu(x, t_f)], \quad (6)$$

with the initial conditions being the fundamental gauge field,

$$B_\mu(x, t_f)|_{t_f=0} = A_\mu(x).$$

A bad approximation: *the diffusion equation*,

$$\frac{\partial}{\partial t_f} B_\mu(x, t_f) \approx \partial^2 B_\mu(x, t_f)$$

The smearing radius increases as $\sqrt{8t_f}$.

24

- The flow equation in the continuum is defined by this differential equation.
- With the covariant derivative given by following, with the \cdot being the derivative with respect to flow time.
- The field strength tensor of the flown fields is given in the regular format.
- The initial condition is the un-flowed gauge field, A_μ .
- Bad approx.: diffusion equation.
- Topological charge preserved and is more pronounced.
- Renormalizes the topological charge at non-zero flow time.

The flow equation

The flow of the SU(3) gauge fields are denoted by $B_\mu(x, t_f)$ which are Lie algebra valued gauge fields,

$$\frac{d}{dt_f} B_\mu(x, t_f) = D_\nu G_{\nu \mu}(x, t_f), \quad (4)$$

$$D_\mu = \partial_\mu + [B_\mu(x, t_f), \cdot], \quad (5)$$

$$G_{\mu\nu}(x, t_f) = \partial_\mu B_\nu(x, t_f) - \partial_\nu B_\mu(x, t_f) - i[B_\mu(x, t_f), B_\nu(x, t_f)], \quad (6)$$

with the initial conditions being the fundamental gauge field,

$$B_\mu(x, t_f)|_{t_f=0} = A_\mu(x).$$

A bad approximation: *the diffusion equation*,

$$\frac{\partial}{\partial t_f} B_\mu(x, t_f) \approx \partial^2 B_\mu(x, t_f)$$

The smearing radius increases as $\sqrt{8t_f}$.

24

- The flow equation in the continuum is defined by this differential equation.
- With the covariant derivative given by following, with the \cdot being the derivative with respect to flow time.
- The field strength tensor of the flown fields is given in the regular format.
- The initial condition is the un-flowed gauge field, A_μ .
- Bad approx.: diffusion equation.
- Topological charge preserved and is more pronounced.
- Renormalizes the topological charge at non-zero flow time.

Gradient flow on the lattice

$$\dot{V}_{tf}(x, \mu) = -g_S^2 \left\{ \partial_{x,\mu} S_G[V_{tf}] \right\} V_{tf}(x, \mu),$$

- On the lattice, the flow equation takes the shape in terms of the link variables.

Gradient flow on the lattice

$$\dot{V}_{tf}(x, \mu) = -g_S^2 \left\{ \partial_{x,\mu} S_G[V_{tf}] \right\} V_{tf}(x, \mu),$$

with initial condition,

$$V_{tf}(x, \mu)|_{t_f=0} = U(x, \mu)$$

- On the lattice, the flow equation takes the shape in terms of the link variables.
- Initial conditions similar to the continuum case.

Gradient flow on the lattice

$$\dot{V}_{tf}(x, \mu) = -g_S^2 \left\{ \partial_{x,\mu} S_G[V_{tf}] \right\} V_{tf}(x, \mu),$$

with initial condition,

$$V_{tf}(x, \mu)|_{t_f=0} = U(x, \mu)$$

Note: need to find the action derivative $S_G[V_{tf}]$.

- On the lattice, the flow equation takes the shape in terms of the link variables.
- Initial conditions similar to the continuum case.
- The action derivative is also needed, but that is a minor task we will not cover here.

Gradient flow on the lattice

$$\dot{V}_{tf}(x, \mu) = -g_S^2 \left\{ \partial_{x,\mu} S_G[V_{tf}] \right\} V_{tf}(x, \mu),$$

with initial condition,

$$V_{tf}(x, \mu)|_{t_f=0} = U(x, \mu)$$

Note: need to find the action derivative $S_G[V_{tf}]$.

- On the lattice, the flow equation takes the shape in terms of the link variables.
- Initial conditions similar to the continuum case.
- The action derivative is also needed, but that is a minor task we will not cover here.

Solving gradient flow with Runge-Kutta 3

With

$$\dot{V}_{tf} = -g_S^2 \left\{ \partial_{x,\mu} S_G[V_{tf}] \right\} V_{tf} = Z(V_{tf}) V_{tf},$$

- We rewrite the equations slightly,

Solving gradient flow with Runge-Kutta 3

With

$$\dot{V}_{tf} = -g_S^2 \left\{ \partial_{x,\mu} S_G[V_{tf}] \right\} V_{tf} = Z(V_{tf}) V_{tf},$$

we get

$$W_0 = V_{tf},$$

$$W_1 = \exp \left[\frac{1}{4} Z_0 \right] W_0,$$

$$W_2 = \exp \left[\frac{8}{9} Z_1 - \frac{17}{36} Z_0 \right] W_1,$$

$$V_{tf+\epsilon_f} = \exp \left[\frac{3}{4} Z_2 - \frac{8}{9} Z_1 + \frac{17}{36} Z_0 \right] W_2,$$

with coefficients from Lüscher [4].

- We rewrite the equations slightly,
- and use a structure preserving integrator with coefficients from Lüscher [4].

Solving gradient flow with Runge-Kutta 3

With

$$\dot{V}_{tf} = -g_S^2 \left\{ \partial_{x,\mu} S_G[V_{tf}] \right\} V_{tf} = Z(V_{tf}) V_{tf},$$

we get

$$W_0 = V_{tf},$$

$$W_1 = \exp \left[\frac{1}{4} Z_0 \right] W_0,$$

$$W_2 = \exp \left[\frac{8}{9} Z_1 - \frac{17}{36} Z_0 \right] W_1,$$

$$V_{tf+\epsilon_f} = \exp \left[\frac{3}{4} Z_2 - \frac{8}{9} Z_1 + \frac{17}{36} Z_0 \right] W_2,$$

with coefficients from Lüscher [4].

26

- We rewrite the equations slightly,
- and use a structure preserving integrator with coefficients from Lüscher [4].
- We control the accuracy of this integrator by ϵ_f .

Solving gradient flow with Runge-Kutta 3

With

$$\dot{V}_{tf} = -g_S^2 \left\{ \partial_{x,\mu} S_G[V_{tf}] \right\} V_{tf} = Z(V_{tf}) V_{tf},$$

we get

$$W_0 = V_{tf},$$

$$W_1 = \exp \left[\frac{1}{4} Z_0 \right] W_0,$$

$$W_2 = \exp \left[\frac{8}{9} Z_1 - \frac{17}{36} Z_0 \right] W_1,$$

$$V_{tf+\epsilon_f} = \exp \left[\frac{3}{4} Z_2 - \frac{8}{9} Z_1 + \frac{17}{36} Z_0 \right] W_2,$$

with coefficients from Lüscher [4].

26

- We rewrite the equations slightly,
- and use a structure preserving integrator with coefficients from Lüscher [4].
- We control the accuracy of this integrator by ϵ_f .

Verifying the integration

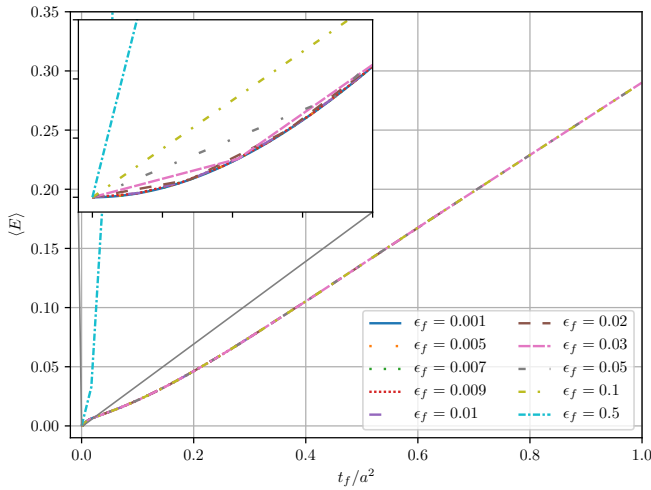
Testing the integrator for different integration steps ϵ_f .

ϵ_f	0.001	0.005	0.007	0.009	0.01	0.02	0.03	0.05	0.1	0.5
--------------	-------	-------	-------	-------	------	------	------	------	-----	-----

- The values we will test the integrator against.

Verifying the integration

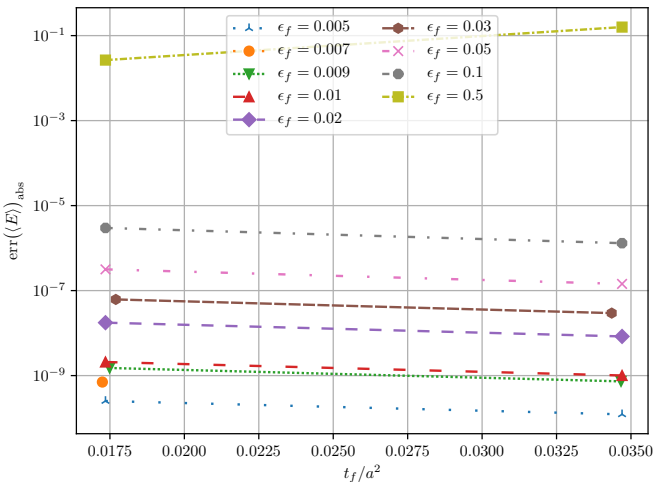
Lattice size $N^3 \times N_T = 24^3 \times 48$ with $\beta = 6.0$.



- The values we will test the integrator against.
- The energy flowed for different the different ϵ_f values.

Verifying the integration

The absolute difference between the smallest flow time $\epsilon_f = 0.001$ and those shown previously.

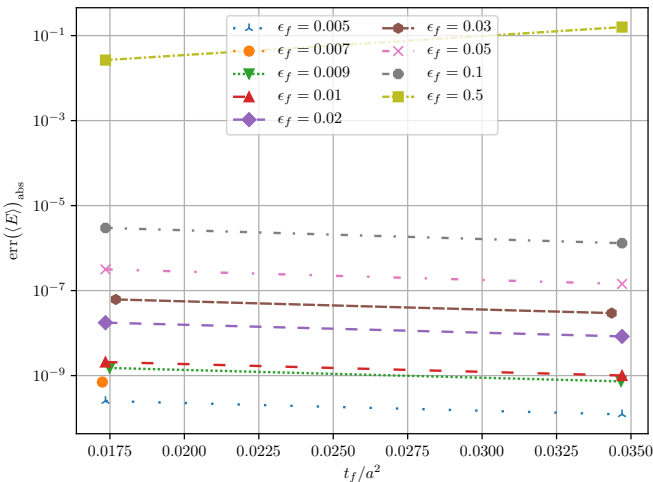


27

- The values we will test the integrator against.
- The energy flowed for different the different ϵ_f values.
- The absolute difference between the smallest flow time $\epsilon_f = 0.001$ and those listed in previous table.
- The reason for **only having two points** is due to the fact that we are **only comparing points** that are **close to each other in flow time**. If we were to have more points, we would have to double the number of flow time steps for the smallest lattices.

Verifying the integration

The absolute difference between the smallest flow time $\epsilon_f = 0.001$ and those shown previously.

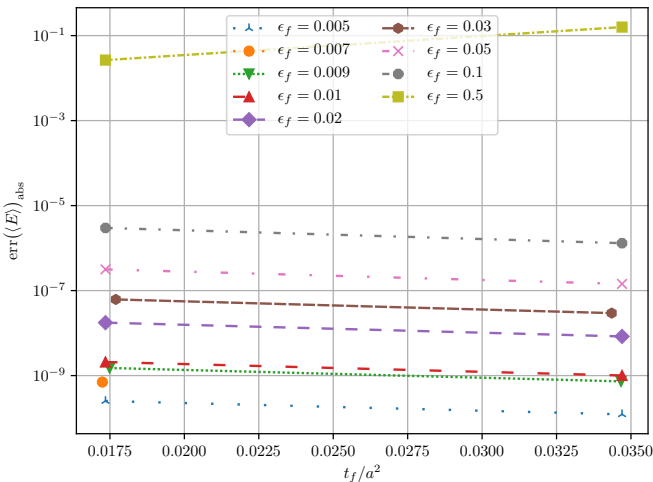


27

- The values we will test the integrator against.
- The energy flowed for different the different ϵ_f values.
- The absolute difference between the smallest flow time $\epsilon_f = 0.001$ and those listed in previous table.
- The reason for **only having two points** is due to the fact that we are **only comparing points** that are **close to each other in flow time**. If we were to have more points, we would have to double the number of flow time steps for the smallest lattices.
- An **example** of the flowing, can be seen by observing the **energy evolving over flow time**.

Verifying the integration

The absolute difference between the smallest flow time $\epsilon_f = 0.001$ and those shown previously.



27

- The values we will test the integrator against.
- The energy flowed for different the different ϵ_f values.
- The absolute difference between the smallest flow time $\epsilon_f = 0.001$ and those listed in previous table.
- The reason for **only having two points** is due to the fact that we are **only comparing points** that are **close to each other in flow time**. If we were to have more points, we would have to double the number of flow time steps for the smallest lattices.
- An **example** of the flowing, can be seen by observing the **energy evolving over flow time**.

Results

Ensembles

Ensemble	β	N	N_T	N_{cfg}	ϵ_{flow}	Config. size[GB]
A	6.0	24	48	1000	0.01	0.356
B	6.1	28	56	1000	0.01	0.659
C	6.2	32	64	2000	0.01	1.125
D_1	6.45	32	32	1000	0.02	0.563
D_2	6.45	48	96	250	0.02	5.695

- We use $N_{\text{corr}} = 1600$ for $\beta = 6.45$ ensembles, $N_{\text{corr}} = 600$ for the rest.

- The main ensembles made for this thesis.
- Every configuration was flown with $N_{\text{flow}} = 1000$ flow steps.
- We should also mention that we generated a few additional ensembles for investigating other aspects of the topological charge.

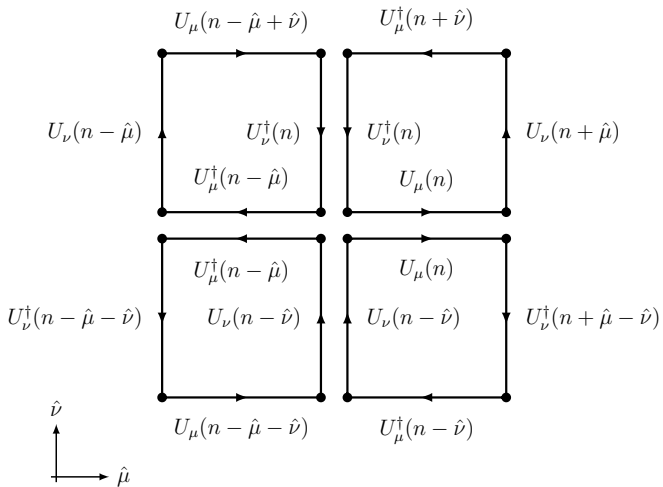
Ensembles

Ensemble	β	N	N_T	N_{cfg}	ϵ_{flow}	Config. size[GB]
A	6.0	24	48	1000	0.01	0.356
B	6.1	28	56	1000	0.01	0.659
C	6.2	32	64	2000	0.01	1.125
D_1	6.45	32	32	1000	0.02	0.563
D_2	6.45	48	96	250	0.02	5.695

- We use $N_{\text{corr}} = 1600$ for $\beta = 6.45$ ensembles, $N_{\text{corr}} = 600$ for the rest.
- $N_{\text{up}} = 30$.

- The main ensembles made for this thesis.
- Every configuration was flown with $N_{\text{flow}} = 1000$ flow steps.
- We should also mention that we generated a few additional ensembles for investigating other aspects of the topological charge.

The clover field strength definition



- We will use the clover field strength definition in gauge observables.

Energy definition

$$E = \frac{a^4}{2|\Lambda|} \sum_{n \in \Lambda} \sum_{\mu, \nu} (F_{\mu\nu}^{\text{clov}}(n))^2$$

30

- We can use this definition to set a scale.

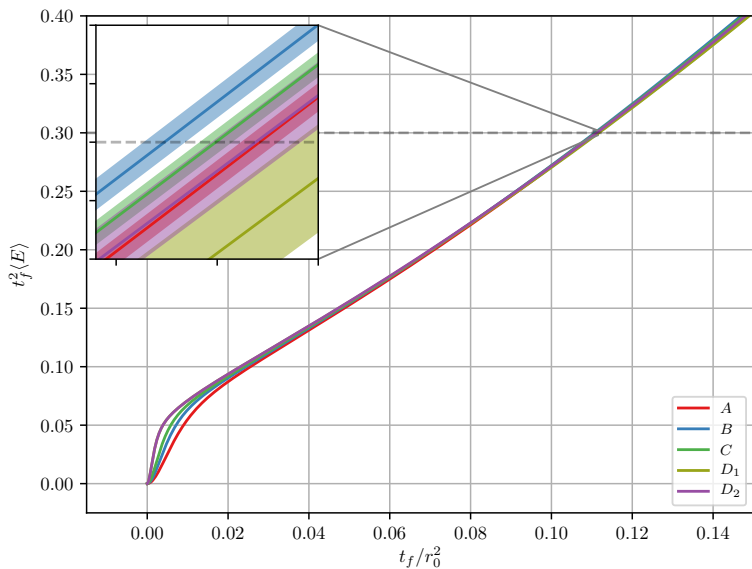
Energy definition

$$E = \frac{a^4}{2|\Lambda|} \sum_{n \in \Lambda} \sum_{\mu, \nu} (F_{\mu\nu}^{\text{clov}}(n))^2$$

We can use this definition to set a scale t_0 ,

$$\left\{ t_f^2 \langle E(t) \rangle \right\}_{t_f=t_0} = 0.3.$$

- We can use this definition to set a scale.



Scale setting t_0

Ensemble	L/a	L [fm]	a [fm]
A	24	2.235(9)	0.0931(4)
B	28	2.214(10)	0.0791(3)
C	32	2.17(1)	0.0679(3)
D_1	32	1.530(9)	0.0478(3)
D_2	48	2.29(1)	0.0478(3)

Scale setting t_0

Ensemble	$t_0[\text{fm}^2]$	t_0/a^2	t_0/r_0^2
A	0.02780(2)	3.20(3)	0.11121(9)
B	0.02769(2)	4.43(4)	0.11075(10)
C	0.02775(2)	6.01(6)	0.11099(8)
D_1	0.02779(5)	12.2(1)	0.1112(2)
D_2	0.02794(9)	12.2(1)	0.1117(3)

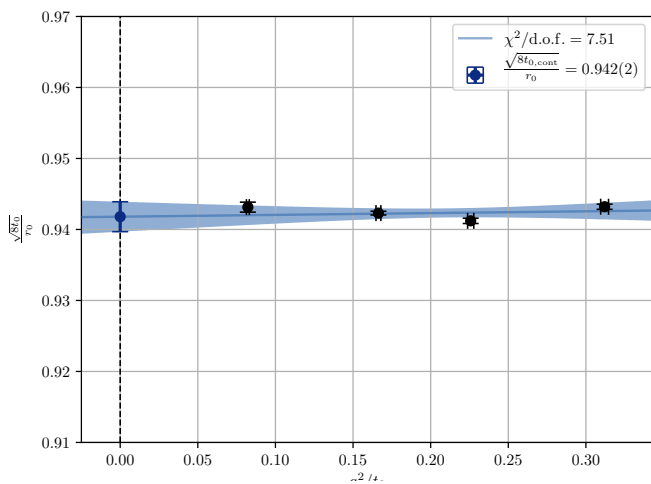
- Extrapolation results for t_0 , where we retrieved the exact point of intersection between $t_f^2 \langle E \rangle$ and 0.3 using $N_{\text{bs}} = 500$ bootstrap fits. Extrapolating to the continuum gives us $t_{0,\text{cont}}/r_0^2 = 0.11087(50)$.

Scale setting t_0

Ensemble	$t_0[\text{fm}^2]$	t_0/a^2	t_0/r_0^2
A	0.02780(2)	3.20(3)	0.11121(9)
B	0.02769(2)	4.43(4)	0.11075(10)
C	0.02775(2)	6.01(6)	0.11099(8)
D_1	0.02779(5)	12.2(1)	0.1112(2)
D_2	0.02794(9)	12.2(1)	0.1117(3)

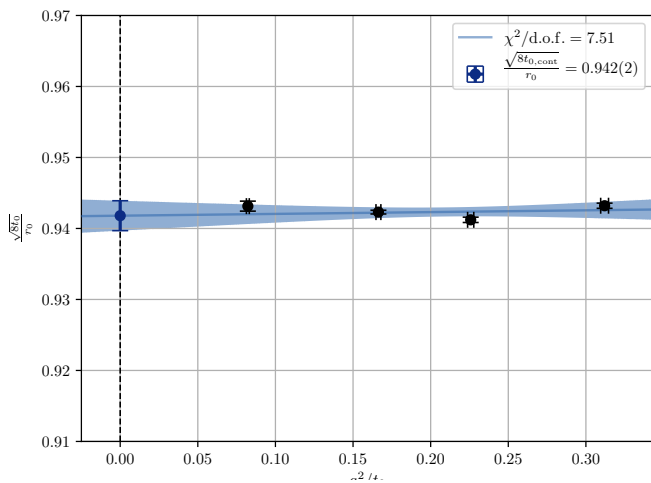
- Extrapolation results for t_0 , where we retrieved the exact point of intersection between $t_f^2 \langle E \rangle$ and 0.3 using $N_{\text{bs}} = 500$ bootstrap fits. Extrapolating to the continuum gives us $t_{0,\text{cont}}/r_0^2 = 0.11087(50)$.

Scale setting t_0



- The continuum extrapolation $a \rightarrow 0$ for t_0 of the four ensembles A , B , C , and D_2 .

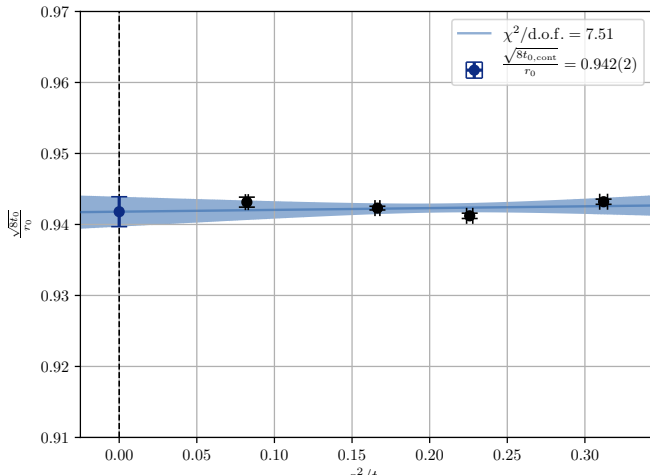
Scale setting t_0



Continuum extrapolation using ensembles A , B , C , and D_2 gives $t_{0,\text{cont}}/r_0^2 = 0.11087(50)$.

- The continuum extrapolation $a \rightarrow 0$ for t_0 of the four ensembles A , B , C , and D_2 .
- $r_0 = 0.5$ fm.

Scale setting t_0



Continuum extrapolation using ensembles A , B , C , and D_2 gives $t_{0,\text{cont}}/r_0^2 = 0.11087(50)$. This matches the values retrieved by Lüscher [4].

- The continuum extrapolation $a \rightarrow 0$ for t_0 of the four ensembles A , B , C , and D_2 .
- $r_0 = 0.5$ fm.

Scale setting t_0

Extrapolations for different ensemble-combinations

Ensembles	$\frac{t_0, \text{cont}}{r_0^2}$	$\chi^2/\text{d.o.f}$
A, B, C, D_2	0.11087(50)	7.51
B, C, D_2	0.1115(3)	0.41
A, B, C, D_1	0.1119(6)	0.88

Scale setting w_0

Can also set a scale using the derivative which offers more granularity for small flow times,

$$W(t)|_{t=w_0^2} = 0.3,$$
$$W(t) \equiv t_f \frac{d}{dt_f} \{ t_f^2 \langle E \rangle \}.$$

Scale setting w_0

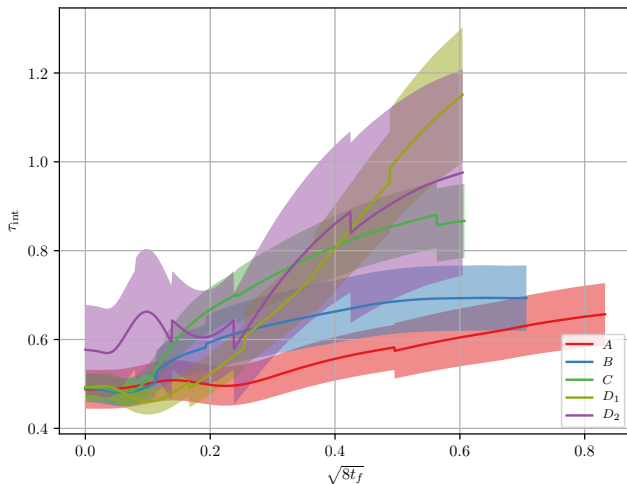
Ensembles	$w_{0\text{cont}}[\text{fm}]$	$\chi^2/\text{d.o.f}$
A, B, C, D_2	0.1695(5)	7.12
B, C, D_2	0.1702(3)	0.53
A, B, C, D_1	0.1706(6)	0.86

Scale setting w_0

Ensembles	$w_{0\text{cont}}[\text{fm}]$	$\chi^2/\text{d.o.f}$
A, B, C, D_2	0.1695(5)	7.12
B, C, D_2	0.1702(3)	0.53
A, B, C, D_1	0.1706(6)	0.86

Comparable to Borsanyi et al. [1] which included dynamical fermions, with $w_{0,\text{cont}} = 0.1755(18)(04)$ fm.

Autocorrelation in the energy



The autocorrelation of the energy. A value of $\tau_{\text{int}} = 0.5$ indicates that we have zero autocorrelation.

Topological charge definition

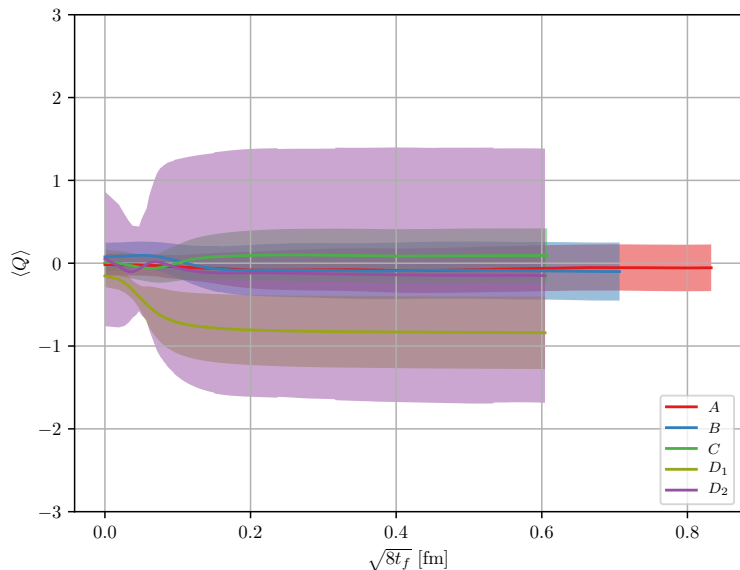
$$Q = a^4 \sum_{n \in \Lambda} q(n),$$

with the charge density given by

$$q(n) = \frac{1}{32\pi^2} \epsilon_{\mu\nu\rho\sigma} \text{tr} [F_{\mu\nu}(n) F_{\rho\sigma}(n)].$$

- We will use the clover field strength definition.
- Symmetries will allow us to reduce the effective number of clovers need to calculate from 24 to 6.

Topological charge



38

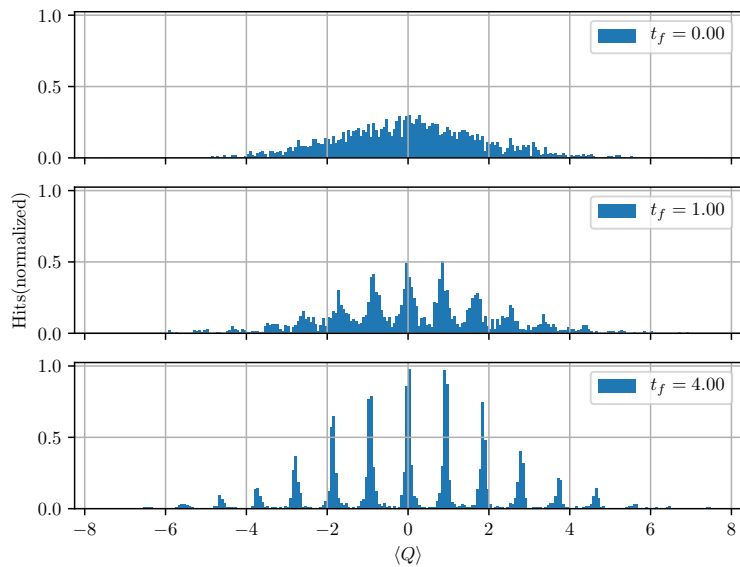
- Topological charge Q as evolved in flow time for the five main ensembles.
- Bootstrapped data with $N_{\text{bs}} = 500$ bootstrap samples.
- Corrected for autocorrelations with $\sigma = \sqrt{2\tau_{\text{int}}}\sigma_0$.

Additional ensembles

Ensemble	N	N_T	N_{cfg}	N_{corr}	N_{up}	a [fm]	L [fm]
E	8	16	8135	600	30	0.0931(4)	0.745(3)
F	12	24	1341	200	20	0.0931(4)	1.118(5)
G	16	32	2000	400	20	0.0790(3)	1.265(6)

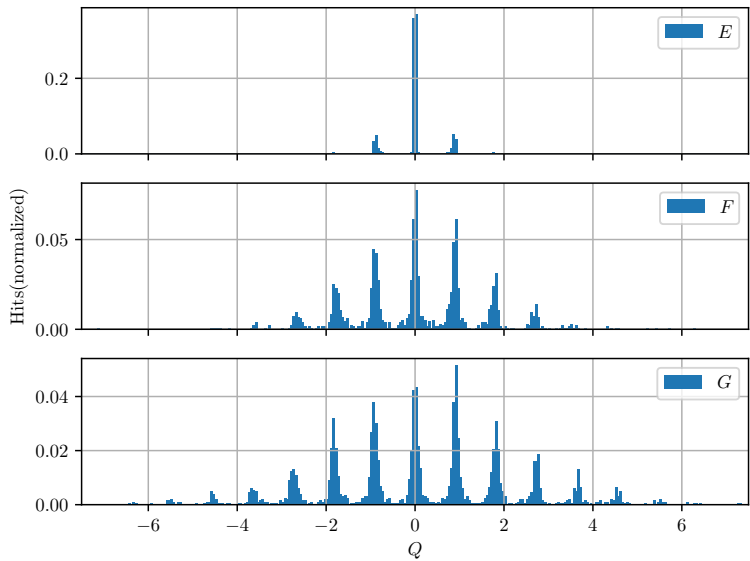
- Additional ensembles made in order to illuminate additional aspects of the topological charge.
- Supporting ensembles made on Smaug. All ensembles were flown $N_{\text{flow}} = 1000$ steps with $\epsilon_{\text{flow}} = 0.01$.

Topological charge distribution



Histograms for the topological charge for ensemble G with a lattice of size $N^3 \times N_T = 16^3 \times 32$ with $\beta = 6.1$, taken at different flow times $t_f/a^2 = 0.0, 1.0, 4.0$ fm.

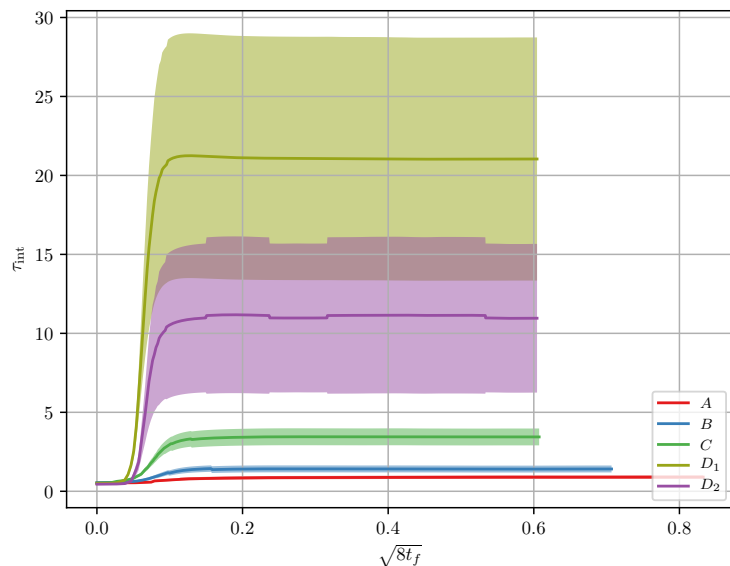
Topological charge distribution in flow time



41

Histograms of topological charge for the supporting ensembles seen at $t_f/a^2 = 0.25$ fm.

Topological charge autocorrelation



The integrated autocorrelation τ_{int} for topological charge for the five main ensembles.

Topological susceptibility

$$\chi_{\text{top}}^{1/4} = \frac{1}{V^{1/4}} \langle Q^2 \rangle^{1/4}$$

43

- We can use the Witten-Veneziano formula in order to extract an estimate for N_f using the topological susceptibility

Topological susceptibility

$$\chi_{\text{top}}^{1/4} = \frac{1}{V^{1/4}} \langle Q^2 \rangle^{1/4}$$

$$m_{\eta'}^2 = \frac{2N_f}{f_\pi^2} \chi_{\text{top}}$$

43

- We can use the Witten-Veneziano formula in order to extract an estimate for N_f using the topological susceptibility
- This can help us understand the "quality" of the ensemble, as we would expect to be around $N_f = 3$.

Topological susceptibility

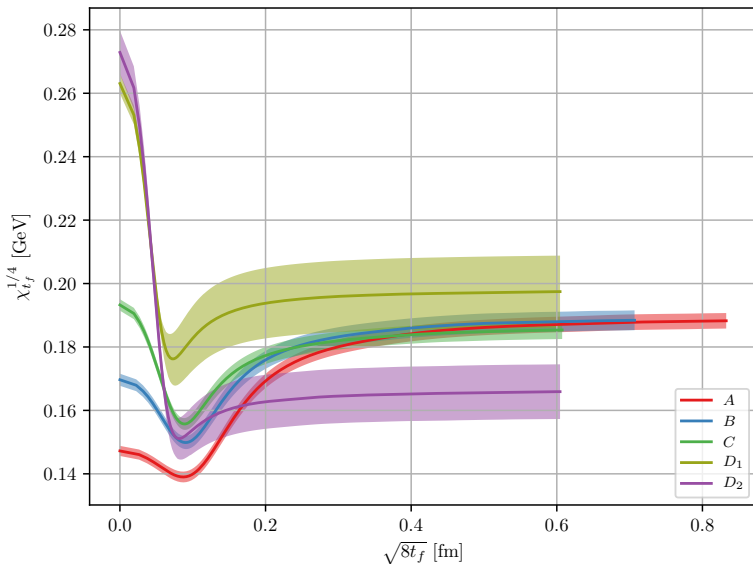
$$\chi_{\text{top}}^{1/4} = \frac{1}{V^{1/4}} \langle Q^2 \rangle^{1/4}$$

$$m_{\eta'}^2 = \frac{2N_f}{f_\pi^2} \chi_{\text{top}}$$

43

- We can use the Witten-Veneziano formula in order to extract an estimate for N_f using the topological susceptibility
- This can help us understand the "quality" of the ensemble, as we would expect to be around $N_f = 3$.

Topological susceptibility



- The topological susceptibility $\chi_{tf}^{1/4}$ of the main ensembles.
- Bootstrapped $N_{\text{bs}} = 500$ times.
- Corrected for autocorrelations with $\sigma = \sqrt{2\tau_{\text{int}}}\sigma_0$.

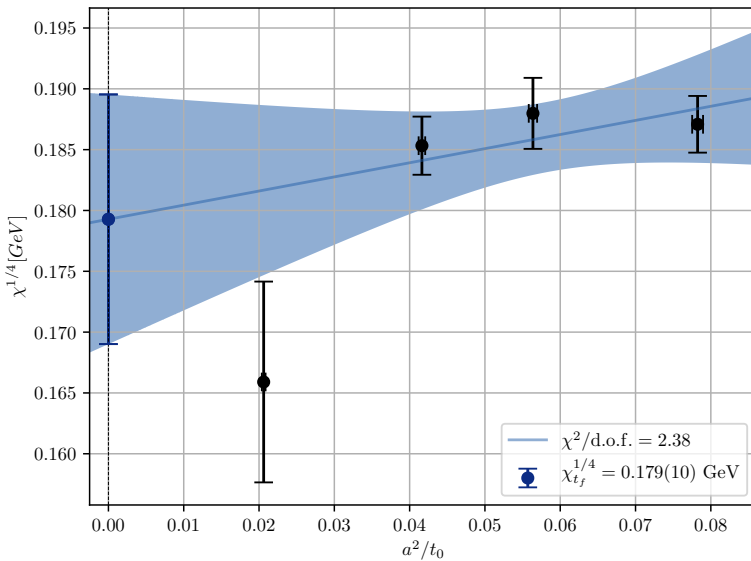
Topological susceptibility continuum extrapolation

Ensemble	$\chi_{tf}^{1/4}$ [GeV]	$\chi_{tf}^{1/4}$ [GeV], corrected	$\sqrt{2\tau_{int}}$
<i>A</i>	0.1877(23)	0.1877(24)	1.028(46)
<i>B</i>	0.1880(21)	0.1880(29)	1.346(81)
<i>C</i>	0.1853(14)	0.1853(24)	1.762(104)
<i>D</i> ₁	0.1971(22)	0.1971(101)	4.523(675)
<i>D</i> ₂	0.1656(33)	0.1656(86)	2.624(441)

Error corrected for autocorrelations with $\sigma = \sqrt{2\tau_{int}}\sigma_0$.

The topological susceptibility for the main ensembles together with the correction factor from the integrated autocorrelation time. The second column have not had its results corrected by $\sqrt{2\tau_{int}}$. None of the results have been analyzed with bootstrapping.

Topological susceptibility continuum extrapolation



46

- A continuum extrapolation of the topological susceptibility $\chi_{tf}^{1/4}$ for the main ensembles excluding the D_1 ensemble.
- The points for $\chi_{tf}^{1/4}$ is taken at $\sqrt{8t_{f,0}} = 0.6 \text{ fm}$.

Topological susceptibility continuum extrapolation

Ensembles	$\chi_{tf}^{1/4} (\langle Q^2 \rangle) [\text{GeV}]$	N_f	$\chi^2/\text{d.o.f}$
A, B, C, D_2	0.179(10)	3.75(29)	2.38
A, B, C, D_1	0.186(6)	3.21(25)	0.83
B, C, D_1	0.187(24)	3.18(24)	1.63
B, C, D_2	0.166(24)	5.06(39)	2.05
A, B, C	0.184(6)	3.37(26)	0.33

The fourth cumulant

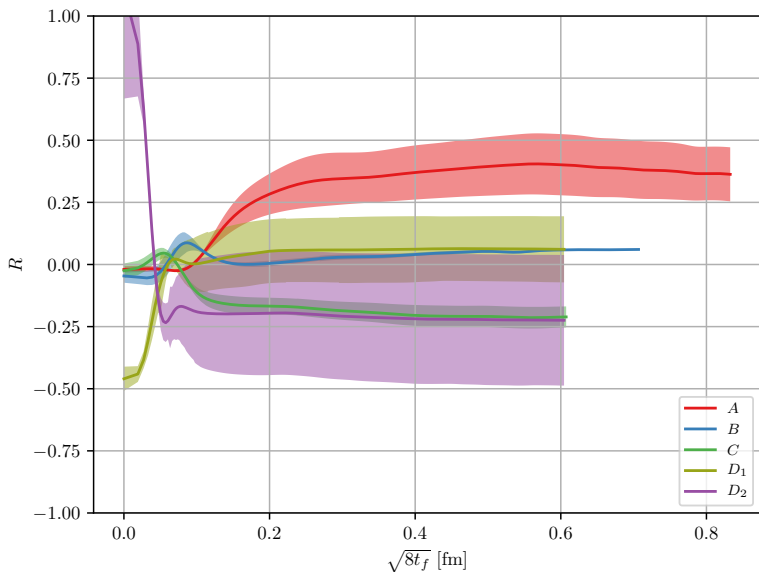
WHAT DO THE R RATIO INDICATE WHEN AWAY FROM ZERO?!

$$\langle Q^4 \rangle_c = \frac{1}{V^2} \left(\langle Q^4 \rangle - 3 \langle Q^2 \rangle^2 \right).$$

From this, we can also measure the ratio R ,

$$R = \frac{\langle Q^4 \rangle_c}{\frac{1}{V} \langle Q^2 \rangle} = \frac{1}{V} \frac{\langle Q^4 \rangle - 3 \langle Q^2 \rangle^2}{\langle Q^2 \rangle},$$

The fourth cumulant



- The fourth cumulant ratio $R = \langle Q^4 \rangle_C / \langle Q^2 \rangle$.
- The results were analyzed using $N_{\text{bs}} = 500$ bootstrap samples, with the error corrected for by $\sqrt{2\tau_{\text{int}}}$.

SCALE THE TABLES

Ensemble	L/a	t_0/a^2	$\langle Q^2 \rangle$	$\langle Q^4 \rangle$	$\langle Q^4 \rangle_C$	
A	2.24	3.20(3)	0.78(4)	2.13(27)	0.282(67)	0.359
B	2.21	4.43(4)	0.81(5)	1.98(23)	0.036(11)	0.044
C	2.17	6.01(6)	0.77(4)	1.6(2)	-0.174(40)	-0.226
D_1	1.53	12.2(1)	1.00(20)	3.01(1.07)	0.03(12)	0.03
D_2	2.29	12.2(1)	0.497(100)	0.64(20)	-0.103(95)	-0.21

The fourth cumulant is taken at their individual reference scales seen in the third column. The data were analyzed with using a bootstrap analysis of $N_{bs} = 500$ samples, with error corrected by the integrated autocorrelation, $\sqrt{2\tau_{int}}$.

Comparing fourth cumulant

WHAT ARTICLE?! SCALE TABLE

Ensemble	β	L/a	L [fm]	a [fm]	t_0/a^2	t_0/r_0^2	
F_1	5.96	16	1.632	0.102	2.7887(2)	0.1113(9)	1 440
B_2	6.05	14	1.218	0.087	3.7960(12)	0.1114(9)	144
\tilde{D}_2		17	1.479		3.7825(8)	0.1110(9)	
B_3	6.13	16	1.232	0.077	4.8855(15)	0.1113(10)	144
\tilde{D}_3		19	1.463		4.8722(11)	0.1110(10)	
B_4	6.21	18	1.224	0.068	6.2191(20)	0.1115(11)	144
\tilde{D}_4		21	1.428		6.1957(14)	0.1111(11)	

- Parameters of the ensembles presented by Cè et al. [2]. The first column is the ensemble name from the article. The letter indicates the volume, while the subindex indicates the β value. Ensembles of similar letters keep approximately the same length L .

Comparing fourth cumulant

WHAT ARTICLE?! SCALE TABLE

Ensemble	$\langle Q^2 \rangle_{\text{normed}}$	$\langle Q^4 \rangle_{\text{normed}}$	$\langle Q^4 \rangle_{C,\text{normed}}$	R_{normed}
F_1	0.728(1)	1.608(4)	0.016(1)	0.022(1)
B_2	0.772(3)	1.873(19)	0.085(4)	0.110(5)
\tilde{D}_2	0.770(3)	1.817(17)	0.037(4)	0.048(5)
B_3	0.760(3)	1.805(17)	0.074(3)	0.097(4)
\tilde{D}_3	0.769(3)	1.801(14)	0.027(1)	0.035(1)
B_4	0.776(3)	1.874(18)	0.069(3)	0.089(4)
\tilde{D}_4	0.785(3)	1.891(17)	0.040(4)	0.052(5)

- Parameters of the ensembles presented by Cè et al. [2]. The first column is the ensemble name from the article. The letter indicates the volume, while the subindex indicates the β value. Ensembles of similar letters keep approximately the same length L .
- Results as presented by Cè et al. [2], normalized by the lattice volume.

Comparing fourth cumulant

WHAT ARTICLE?! SCALE TABLE

Article	Thesis	Ratio($\langle Q^2 \rangle$)	Ratio($\langle Q^4 \rangle$)	Ratio($\langle Q^4 \rangle_C$)	Ratio(R)
F_1	A	1.08(6)	1.34(18)	19.03(5.81)	17.64(4.48)
B_2	A	1.02(5)	1.15(15)	3.60(1.09)	3.54(90)
	B	1.04(6)	1.06(11)	0.480(74)	0.46(4)
\tilde{D}_2	A	1.02(5)	1.19(15)	8.31(1.99)	8.15(1.56)
	B	1.05(6)	1.10(12)	1.1(1)	1.06(3)
B_3	B	1.06(6)	1.10(12)	0.550(86)	0.52(5)
\tilde{D}_3	B	1.05(6)	1.11(12)	1.51(23)	1.4(1)
B_4	C	0.99(5)	0.86(8)	-2.32(46)	-2.35(59)
\tilde{D}_4	C	0.98(5)	0.85(8)	-3.95(96)	-4.05(1.19)

51

- Parameters of the ensembles presented by Cè et al. [2]. The first column is the ensemble name from the article. The letter indicates the volume, while the subindex indicates the β value. Ensembles of similar letters keep approximately the same length L .
- Results as presented by Cè et al. [2], normalized by the lattice volume.
- A comparison between the results obtained in this thesis on the fourth cumulant, and by those similar in volume form Cè et al. [2]. *Ratio* indicates that we are dividing our results by the ones in previous table.

WHAT ARTICLE?! SCALE TABLE

51

- Parameters of the ensembles presented by Cè et al. [2]. The first column is the ensemble name from the article. The letter indicates the volume, while the subindex indicates the β value. Ensembles of similar letters keep approximately the same length L .
- Results as presented by Cè et al. [2], normalized by the lattice volume.
- A comparison between the results obtained in this thesis on the fourth cumulant, and by those similar in volume form Cè et al. [2]. *Ratio* indicates that we are dividing our results by the ones in previous table.

The topological charge correlator

CLEAN UP! REMOVE GENERAL EXPRESSION(ITS JUST MORE CONFUSING!)EXPLAIN HERE WHAT SOURCE/SINK IS
A general correlator is given as,

$$C(n_t) = \left\langle \hat{O}_2(\mathbf{0}, n_t) \hat{O}_1(\mathbf{0}, 0) \right\rangle = \sum_k \langle 0 | \hat{O}_2 | k \rangle \langle k | \hat{O}_1 | 0 \rangle e^{-n_t E_k}$$

where n_t is the Euclidean time in which the correlator is taken and E_k is states of energy.

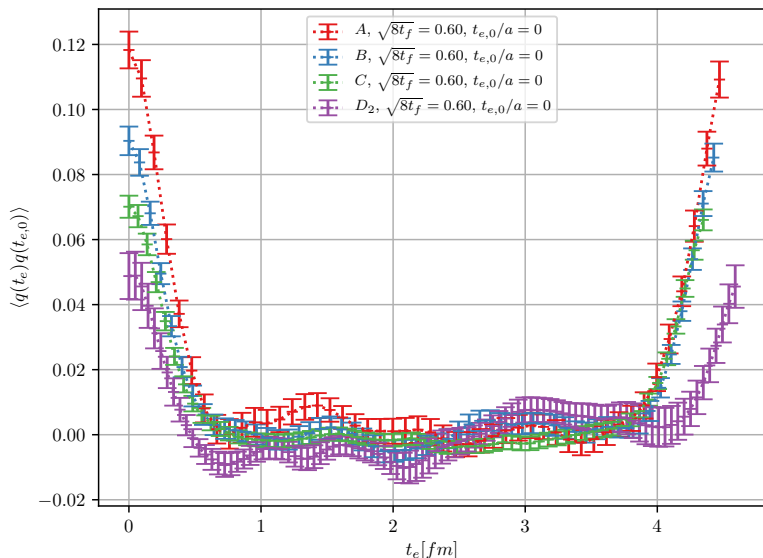
The topological charge correlator

$$C(n_t) = \langle q(n_t) q(0) \rangle,$$

$q(0)$ is the *source* and $q(n_t)$ is the *sink*.

- $q(0)$ is not required to be at $n_t = 0$.

The topological charge correlator



53

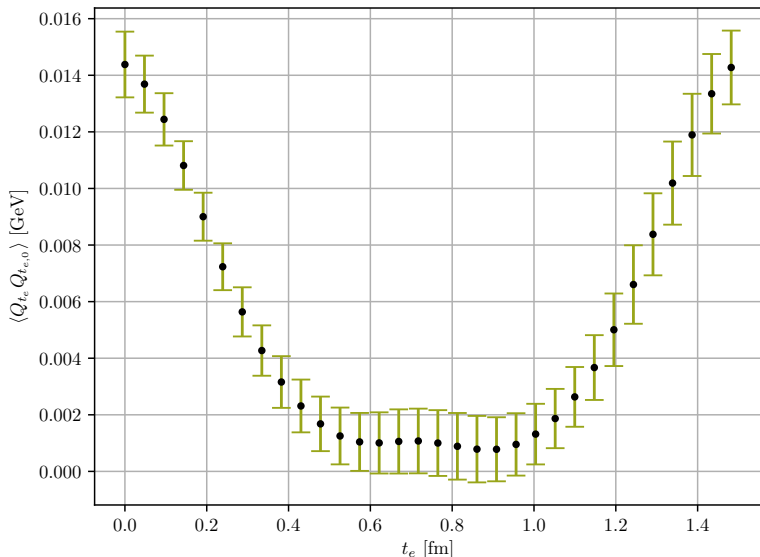
- The topological charge correlator for all of the ensembles except D_1 . The x -axis contains the sink-source separation, as the source $q(0)$ is placed at $t_e = 0$ fm, and the sink $q(t_e)$ is taken at t_e .

The topological charge correlator

53

- The topological charge correlator for all of the ensembles except D_1 . The x -axis contains the sink-source separation, as the source $q(0)$ is placed at $t_e = 0$ fm, and the sink $q(t_e)$ is taken at t_e .
- We since the ensembles are of different lattice sizes, we plot th D_1 separately.

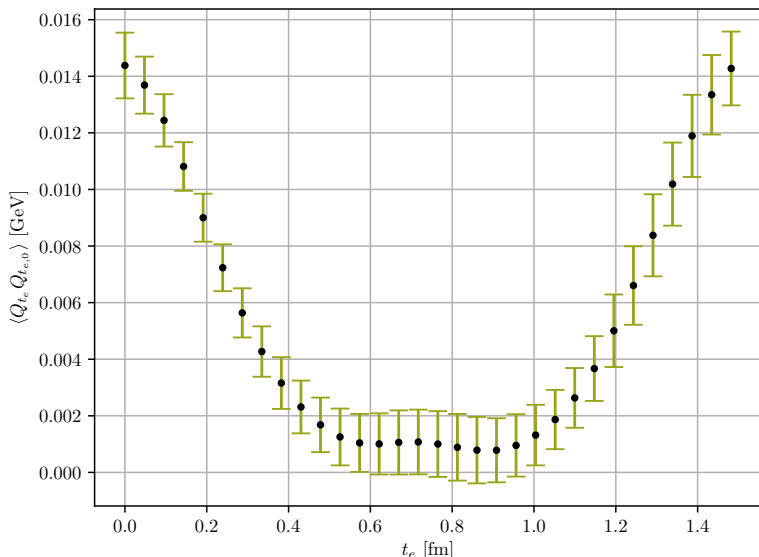
The topological charge correlator



53

- The topological charge correlator for all of the ensembles except D_1 . The x -axis contains the sink-source separation, as the source $q(0)$ is placed at $t_e = 0$ fm, and the sink $q(t_e)$ is taken at t_e .
- We since the ensembles are of different lattice sizes, we plot th D_1 separately.
- The topological charge correlator for the D_1 . The source $q(0)$ is placed at $t_e = 0$ fm and the sink $q(t_e)$ is taken at t_e .

The topological charge correlator



53

- The topological charge correlator for all of the ensembles except D_1 . The x -axis contains the sink-source separation, as the source $q(0)$ is placed at $t_e = 0$ fm, and the sink $q(t_e)$ is taken at t_e .
- We since the ensembles are of different lattice sizes, we plot th D_1 separately.
- The topological charge correlator for the D_1 . The source $q(0)$ is placed at $t_e = 0$ fm and the sink $q(t_e)$ is taken at t_e .

The effective glueball mass

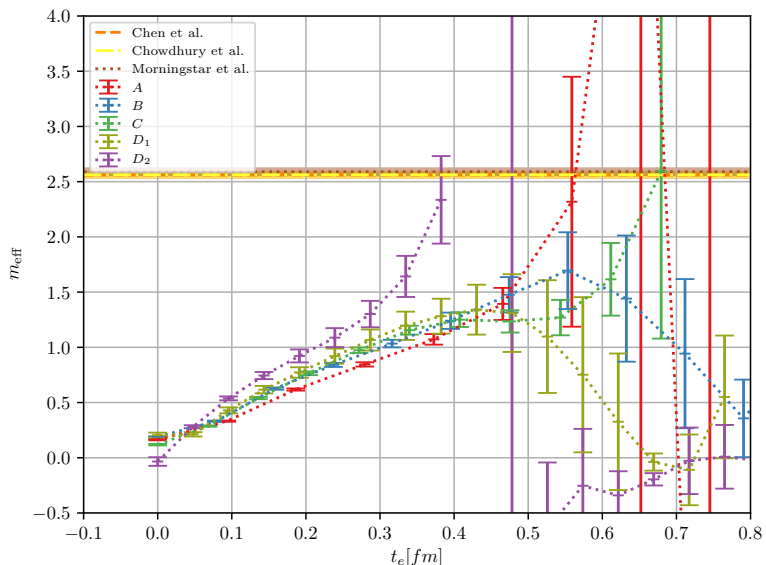
The ground state in the correlator is given as

$$C(n_t) = A_0 e^{-n_t E_0} + A_1 e^{-n_t E_1} + \dots$$

which can be extracted as

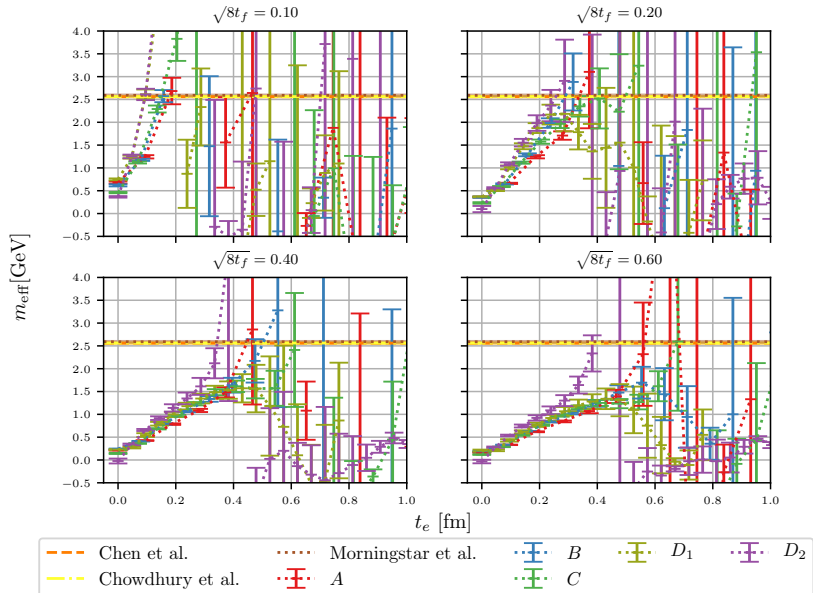
$$am_{\text{eff}} = \log \left(\frac{C(n_t)}{C(n_t + 1)} \right),$$

The effective glueball mass



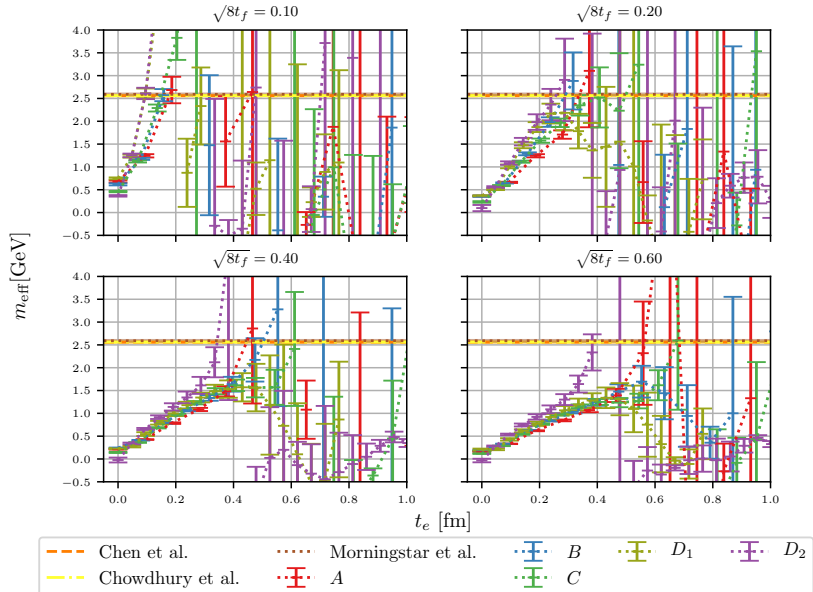
- The effective mass of the glueball, as extracted from the topological charge correlator in Euclidean time.

The effective glueball mass



- ~~CLEAN UP COMMENT ON FRAME!~~ The effective mass of the glueball charge correlator in Euclidean time, seen at four different flow times, $\sqrt{8t_{f,0}} \in [0.1, 0.2, 0.3, 0.4, 0.6]$.
- Low statistics and critical slowdown \rightarrow poor signal.

The effective glueball mass



- ~~CLEAN UP COMMENT ON FRAME!~~ The effective mass of the glueball charge correlator in Euclidean time, seen at four different flow times, $\sqrt{8t_{f,0}} \in [0.1, 0.2, 0.3, 0.4, 0.6]$.
- Low statistics and critical slowdown \rightarrow poor signal.

Conclusion, future developments and final thoughts

Conclusion

- Scaling and parameter optimizations

56

- Checked scaling and parameter optimization.

Conclusion

- Scaling and parameter optimizations
 - Room for increased processors.

56

- Checked scaling and parameter optimization.
- We checked **strong**, **weak** and **speedup**, where we appeared to have a plateauing around 512 processors but with room for optimization.

Conclusion

- Scaling and parameter optimizations
 - Room for increased processors.
 - $N_{\text{up}} > N_{\text{corr}}$

56

- Checked scaling and parameter optimization.
- We checked **strong**, **weak** and **speedup**, where we appeared to have a plateauing around 512 processors but with room for optimization.
- N_{up} could be increased, as it has a smaller impact than N_{corr} .

Conclusion

- Scaling and parameter optimizations
 - Room for increased processors.
 - $N_{\text{up}} > N_{\text{corr}}$
 - Machine precision accuracy when comparing with Chroma.

56

- Checked scaling and parameter optimization.
- We checked **strong**, **weak** and **speedup**, where we appeared to have a plateauing around 512 processors but with room for optimization.
- N_{up} could be increased, as it has a smaller impact than N_{corr} .
- Same results as Chroma down to machine precision.
- We also checked the ϵ_{rnd} for matrix generation parameter that it minimized the autocorrelation, and the integration step ϵ_f .

Conclusion

- Scaling and parameter optimizations
 - Room for increased processors.
 - $N_{\text{up}} > N_{\text{corr}}$
 - Machine precision accuracy when comparing with Chroma.
- t_0 and w_0 match other papers, e.g. Lüscher [4] and Cè et al. [2].

56

- Checked scaling and parameter optimization.
- We checked **strong**, **weak** and **speedup**, where we appeared to have a plateauing around 512 processors but with room for optimization.
- N_{up} could be increased, as it has a smaller impact than N_{corr} .
- Same results as Chroma down to machine precision.
- We also checked the ϵ_{rnd} for matrix generation parameter that it minimized the autocorrelation, and the integration step ϵ_f .
- t_0 and w_0 match other papers.

Conclusion

- Scaling and parameter optimizations
 - Room for increased processors.
 - $N_{\text{up}} > N_{\text{corr}}$
 - Machine precision accuracy when comparing with Chroma.
- t_0 and w_0 match other papers, e.g. Lüscher [4] and Cè et al. [2].
- $\langle Q \rangle \neq 0$ for some ensembles.

56

- Checked scaling and parameter optimization.
- We checked **strong**, **weak** and **speedup**, where we appeared to have a plateauing around 512 processors but with room for optimization.
- N_{up} could be increased, as it has a smaller impact than N_{corr} .
- Same results as Chroma down to machine precision.
- We also checked the ϵ_{rnd} for matrix generation parameter that it minimized the autocorrelation, and the integration step ϵ_f .
- t_0 and w_0 match other papers.
- $\langle Q \rangle$

Conclusion

- Scaling and parameter optimizations
 - Room for increased processors.
 - $N_{\text{up}} > N_{\text{corr}}$
 - Machine precision accuracy when comparing with Chroma.
- t_0 and w_0 match other papers, e.g. Lüscher [4] and Cè et al. [2].
- $\langle Q \rangle \neq 0$ for some ensembles.
- The topological susceptibility $\langle \chi_f^{1/4} \rangle$ and N_f

56

- Checked scaling and parameter optimization.
- We checked **strong**, **weak** and **speedup**, where we appeared to have a plateauing around 512 processors but with room for optimization.
- N_{up} could be increased, as it has a smaller impact than N_{corr} .
- Same results as Chroma down to machine precision.
- We also checked the ϵ_{rnd} for matrix generation parameter that it minimized the autocorrelation, and the integration step ϵ_f .
- t_0 and w_0 match other papers.
- $\langle Q \rangle$
- $\chi_f^{1/4}$. Matches well with other papers

Conclusion

- Scaling and parameter optimizations
 - Room for increased processors.
 - $N_{\text{up}} > N_{\text{corr}}$
 - Machine precision accuracy when comparing with Chroma.
- t_0 and w_0 match other papers, e.g. Lüscher [4] and Cè et al. [2].
- $\langle Q \rangle \neq 0$ for some ensembles.
- The topological susceptibility $\langle \chi_f^{1/4} \rangle$ and N_f
- $\langle Q^4 \rangle_C$ and R . Sensitive quantities - need large statistics.

56

- Checked scaling and parameter optimization.
- We checked **strong**, **weak** and **speedup**, where we appeared to have a plateauing around 512 processors but with room for optimization.
- N_{up} could be increased, as it has a smaller impact than N_{corr} .
- Same results as Chroma down to machine precision.
- We also checked the ϵ_{rnd} for matrix generation parameter that it minimized the autocorrelation, and the integration step ϵ_f .
- t_0 and w_0 match other papers.
- $\langle Q \rangle$
- $\chi_f^{1/4}$. Matches well with other papers
- $\langle Q^4 \rangle_C$ and R . Sensitive quantity, matches well of first and second moment.

Conclusion

- Scaling and parameter optimizations
 - Room for increased processors.
 - $N_{\text{up}} > N_{\text{corr}}$
 - Machine precision accuracy when comparing with Chroma.
- t_0 and w_0 match other papers, e.g. Lüscher [4] and Cè et al. [2].
- $\langle Q \rangle \neq 0$ for some ensembles.
- The topological susceptibility $\langle \chi_f^{1/4} \rangle$ and N_f
- $\langle Q^4 \rangle_C$ and R . Sensitive quantities - need large statistics.
- Topological charge correlator $\langle q(n_t)q(0) \rangle$ and glueball mass.

56

- Checked scaling and parameter optimization.
- We checked **strong**, **weak** and **speedup**, where we appeared to have a plateauing around 512 processors but with room for optimization.
- N_{up} could be increased, as it has a smaller impact than N_{corr} .
- Same results as Chroma down to machine precision.
- We also checked the ϵ_{rnd} for matrix generation parameter that it minimized the autocorrelation, and the integration step ϵ_f .
- t_0 and w_0 match other papers.
- $\langle Q \rangle$
- $\chi_f^{1/4}$. Matches well with other papers
- $\langle Q^4 \rangle_C$ and R . Sensitive quantity, matches well of first and second moment.
- Topological charge correlator $\langle q(n_t)q(0) \rangle$ and glueball mass.

Conclusion

- Scaling and parameter optimizations
 - Room for increased processors.
 - $N_{\text{up}} > N_{\text{corr}}$
 - Machine precision accuracy when comparing with Chroma.
- t_0 and w_0 match other papers, e.g. Lüscher [4] and Cè et al. [2].
- $\langle Q \rangle \neq 0$ for some ensembles.
- The topological susceptibility $\langle \chi_f^{1/4} \rangle$ and N_f
- $\langle Q^4 \rangle_C$ and R . Sensitive quantities - need large statistics.
- Topological charge correlator $\langle q(n_t)q(0) \rangle$ and glueball mass.
- Statistics, autocorrelation and critical slowdown.

56

- Checked scaling and parameter optimization.
- We checked **strong**, **weak** and **speedup**, where we appeared to have a plateauing around 512 processors but with room for optimization.
- N_{up} could be increased, as it has a smaller impact than N_{corr} .
- Same results as Chroma down to machine precision.
- We also checked the ϵ_{rnd} for matrix generation parameter that it minimized the autocorrelation, and the integration step ϵ_f .
- t_0 and w_0 match other papers.
- $\langle Q \rangle$
- $\chi_f^{1/4}$. Matches well with other papers
- $\langle Q^4 \rangle_C$ and R . Sensitive quantity, matches well of first and second moment.
- Topological charge correlator $\langle q(n_t)q(0) \rangle$ and glueball mass.
- Critical slowdown, which makes transitioning to a new, independent configuration difficult. This inhibits the gathering of statistics, and helps us explain why we for larger β values have fewer independent gauge configurations.

Conclusion

- Scaling and parameter optimizations
 - Room for increased processors.
 - $N_{\text{up}} > N_{\text{corr}}$
 - Machine precision accuracy when comparing with Chroma.
- t_0 and w_0 match other papers, e.g. Lüscher [4] and Cè et al. [2].
- $\langle Q \rangle \neq 0$ for some ensembles.
- The topological susceptibility $\langle \chi_f^{1/4} \rangle$ and N_f
- $\langle Q^4 \rangle_C$ and R . Sensitive quantities - need large statistics.
- Topological charge correlator $\langle q(n_t)q(0) \rangle$ and glueball mass.
- Statistics, autocorrelation and critical slowdown.

56

- Checked scaling and parameter optimization.
- We checked **strong**, **weak** and **speedup**, where we appeared to have a plateauing around 512 processors but with room for optimization.
- N_{up} could be increased, as it has a smaller impact than N_{corr} .
- Same results as Chroma down to machine precision.
- We also checked the ϵ_{rnd} for matrix generation parameter that it minimized the autocorrelation, and the integration step ϵ_f .
- t_0 and w_0 match other papers.
- $\langle Q \rangle$
- $\chi_f^{1/4}$. Matches well with other papers
- $\langle Q^4 \rangle_C$ and R . Sensitive quantity, matches well of first and second moment.
- Topological charge correlator $\langle q(n_t)q(0) \rangle$ and glueball mass.
- Critical slowdown, which makes transitioning to a new, independent configuration difficult. This inhibits the gathering of statistics, and helps us explain why we for larger β values have fewer independent gauge configurations.

Future developments and final thoughts

- Better statistics.

Future developments and final thoughts

- Better statistics.
- Better utilization of support ensembles E , F and G .

Future developments and final thoughts

- Better statistics.
- Better utilization of support ensembles E , F and G .
- Improve autocorrelation with larger N_{up} .

Future developments and final thoughts

- Better statistics.
- Better utilization of support ensembles E , F and G .
- Improve autocorrelation with larger N_{up} .
- Implement better actions with and operators containing errors.

Future developments and final thoughts

- Better statistics.
- Better utilization of support ensembles E , F and G .
- Improve autocorrelation with larger N_{up} .
- Implement better actions with and operators containing errors.
- Fermions and HMC(Hybrid Monte Carlo).

FIX THIS! 5.0pt

Questions?

-
- [1] S. Borsanyi, S. Durr, Z. Fodor, C. Hoelbling, S. D. Katz, S. Krieg, T. Kurth, L. Lellouch, T. Lippert, C. McNeile, and K. K. Szabo. High-precision scale setting in lattice QCD. *Journal of High Energy Physics*, 2012(9), September 2012. ISSN 1029-8479. doi: 10.1007/JHEP09(2012)010. URL <http://arxiv.org/abs/1203.4469>. arXiv: 1203.4469.
 - [2] Marco Cè, Cristian Consonni, Georg P. Engel, and Leonardo Giusti. Non-Gaussianities in the topological charge distribution of the SU(3) Yang–Mills theory. *Physical Review D*, 92(7), October 2015. ISSN 1550-7998, 1550-2368. doi: 10.1103/PhysRevD.92.074502. URL <http://arxiv.org/abs/1506.06052>. arXiv: 1506.06052.
 - [3] Hilmar Forkel. A Primer on Instantons in QCD. *arXiv:hep-ph/0009136*, September 2000. URL <http://arxiv.org/abs/hep-ph/0009136>. arXiv: hep-ph/0009136.
 - [4] Martin Lüscher. Properties and uses of the Wilson flow in lattice QCD. *Journal of High Energy Physics*, 2010(8), August 2010. ISSN 1029-8479. doi: 10.1007/JHEP08(2010)071. URL <http://arxiv.org/abs/1006.4518>. arXiv: 1006.4518.